Measurement and tuning of the chromatic dispersion of a silicon photonic wire around the half band gap spectral region

François Leo,* Utsav Dave, Shahram Keyvaninia, Bart Kuyken, and Gunther Roelkens

Photonics Research Group—Center for nano- and biophotonics (NB-Photonics), Sint-Pietersnieuwstraat 41, B-9000 Ghent, Belgium
**Corresponding author: francois.leo@intec.ugent.be*

Received October 24, 2013; revised December 6, 2013; accepted December 6, 2013;
posted December 13, 2013 (Doc. ID 200060); published January 31, 2014

We demonstrate the measurement and tuning of second-to-fourth order dispersion of a silicon wire waveguide in a spectral region of low nonlinear losses. Using white light interferometry we extract the chromatic dispersion of our waveguide from 1950 to 2300 nm. Moreover we demonstrate tuning of the zero dispersion wavelength over more than 100 nm, pushing it to longer wavelength by partially underetching the waveguide. © 2014 Optical Society of America

OCIS codes: (130.4310) Nonlinear; (260.2030) Dispersion.
http://dx.doi.org/10.1364/OL.39.000711

Nonlinear silicon photonics is attracting a lot of attention because of its possible application to high-speed signal processing and spectroscopy [1]. Because of the high confinement offered by the silicon-on-insulator (SOI) platform (as a result of the high index contrast between silicon and silica) and the intrinsically high nonlinear index of silicon, nonlinear parameters 5 orders of magnitude higher than standard optical fibers have been reported [2]. However, in order to fully benefit from such high nonlinearity, one should work above the half band gap spectral region, i.e., $\lambda > 2.2$ μm, where two-photon absorption-based nonlinear losses significantly drop [3]. Recent results such as parametric amplification [4] and supercontinuum generation [5] have confirmed the large potential of this spectral region. Most nonlinear processes require good tailoring of the group velocity dispersion of the guided mode. Anomalous dispersion is necessary to achieve phase matching for parametric amplification or to reach solitonic propagation [6]. Strong modal confinement is necessary to achieve such anomalous regime as the material dispersion of silicon is strongly normal [7]. Here we focus on photonic wire waveguides with a standard silicon waveguide layer thickness of 220 nm, easily available through cost-sharing platforms such as epixfab [8]. Moreover, it is in such waveguides that a record nonlinear parameter of 150 $(\mathrm{Wm})^{-1}$ was recently reported in the half band-gap spectral region [9]. Full-vectorial mode solver simulations show that the region of anomalous dispersion is highly sensitive to silicon waveguide layer thickness and waveguide width. Optimal operation for 220 nm silicon thickness is found for a waveguide width of 900 nm, with an anomalous region extending up to 2400 nm [5] However, waveguide widths and especially silicon waveguide layer thickness can vary within a wafer and from wafer to wafer, which can lead to very different dispersion profiles than expected and is detrimental for nonlinear applications. In this paper, we adapt a well-known interferometric method used for fibers [10] to measure the dispersion in these wire waveguides. Previous measurements of the dispersion of silicon waveguides, using either white-light interferometry [11,12] or integrated Mach–Zehnder interferometers [13], were limited to a narrow telecom band. Here we show that such a technique can be easily adapted to any spectral region where broadband sources and detectors are available. We demonstrate measurements of second to fourth order dispersion from 1950 nm up to 2300 nm, a wavelength range of particular interest for nonlinear optics as discussed above. Moreover, we propose underetching as a technique to tune the anomalous region to longer wavelength. Dispersion tailoring and tuning of nanophotonic waveguides for nonlinear optics applications has been intensely studied in recent years. Tuning was performed by depositing dielectric overlayers through chemical vapor deposition [14] or atomic layer deposition [15]. However such techniques decrease the vertical confinement, which do not allow tuning the anomalous region to a longer wavelength in this case. Here we use underetching, i.e., removing the silicon dioxide by wet etching, in order to increase the vertical confinement of the optical mode and shift the zero dispersion wavelength (ZDW) to longer wavelengths. There are two other advantages of this technique compared to the deposition of dielectric overlayers: firstly, the possibility to very precisely control the etch rate and hence the undercut (a rate of 1 nm/min was achieved); secondly, the modal confinement is increased, thereby increasing the nonlinear parameter of the waveguide. Our measurement setup is depicted in Fig. 1. It consists of a Mach–Zehnder interferometer with an air path in one arm and a silicon waveguide in the other. The length of the air arm is chosen so that the group delay is the same in both arms. The fringe spacing of the output interferogram then depends only on higher order dispersion, which can be extracted by careful fitting [10]. The interferometer is stabilized by a feedback loop using a single wavelength 1550 nm laser and a piezo controller mounted on one of the collimators of the air arm. We use two different light sources: the CW amplified spontaneous emission (ASE) from a Cr^{2+}:ZnSe laser that extends from 2050 to 2400 nm and a nanosecond pulsed supercontinuum source that extends from 1950 to 2350 nm. The coupling to the silicon waveguide is performed using lensed fibers. We use a 2 cm long,

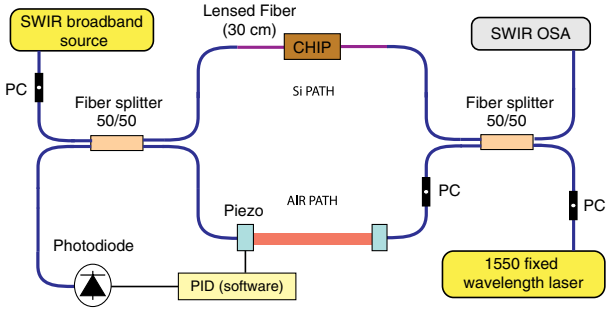

Fig. 1. Experimental setup used to measure the chromatic dispersion. It consists of a stabilized Mach–Zehnder interferometer with a tunable air path in one arm and a silicon waveguide in the other. SWIR: short-wave infared, OSA: optical spectrum analyzer, PC: polarization controller. PD: photodiode, PID: proportional-integral-derivative controller. As a broadband source, an IPG laser and an advalue photonics supercontinuum source (AP-SC-MIR) is used. A Yokogawa AQ6375 SWIR spectrum analyzer is used.

nominally 850 nm wide silicon waveguide that is adiabatically tapered to a width of 3 μm to increase the overlap with the mode of the lensed fibers. This 3 μm waveguide is 4 mm long and exhibits very large normal dispersion ($\beta_2 \approx 3$ ps^2/m) so the accumulated dispersion is of the same order of magnitude as the one expected from the 2 cm long waveguide. The total measured dispersion would therefore be very low and hence difficult to extract. In order to circumvent this problem, we measured the dispersion of a waveguide that consists of the tapers only and added standard SMF fiber (anomalous in that wavelength region) in order to reduce as much as possible the average group-velocity dispersion of the reference in the spectral region of interest. The experiment is then performed in two steps. First we measure the reference waveguide that consists of the tapers only. Then we measure our 2 cm long waveguide and obtain our results by subtracting the total dispersion of both measurements. In order to extract the dispersion parameters from the interferogram, we mathematically describe it as in [10]:

$$I_{\text{out}}(\omega) = I_{\text{air}}(\omega) + I_{\text{wav}}(\omega) + 2V\sqrt{I_{\text{air}}(\omega)I_{\text{wav}}(\omega)}\cos(\phi(\omega)), \quad (1)$$

$$\phi(\omega) = \frac{\omega}{c}l_{\text{air}} - \beta(\omega)l_{\text{wav}}, \quad (2)$$

where l_{air} and l_{wav} are the length of the air and waveguide arms and I_{air} (resp. I_{wav}) is the spectrum at the output of the interferometer when the waveguide (resp. air) arm is blocked. We consider here a coherence function V [16] that does not depend on the frequency. By introducing the standard Taylor expansion of the dispersion characteristics of the guided mode [6] in Eq. (2), we find

$$\phi(\Omega) = \left(\frac{\omega_0 l_{\text{air}}}{c} - l_{\text{wav}}\beta_0\right) + \Omega\left(\frac{l_{\text{air}}}{c} - l_{\text{wav}}\beta_1\right) - l_{\text{wav}}\left(\frac{1}{2}\beta_2\Omega^2 + \frac{1}{6}\beta_3\Omega^3 + \frac{1}{24}\beta_4\Omega^4 \ldots\right), \quad (3)$$

where we introduced the frequency shift $\Omega = \omega - \omega_0$. Choosing ω_0 such $l_{\text{air}}/c = l_{\text{wav}}\beta_1$, i.e., canceling the group delay difference between the two arms, the second term from the right hand side cancels and we finally obtain

$$I_{\text{out}}(\Omega) = I_{\text{air}}(\Omega) + I_{\text{wav}}(\Omega) + 2V\sqrt{I_{\text{air}}(\Omega)I_{\text{wav}}(\Omega)}\cos(\phi(\Omega)) \quad (4)$$

$$\phi(\Omega) = C - l_{\text{wav}}\left(\frac{1}{2}\beta_2\Omega^2 + \frac{1}{6}\beta_3\Omega^3 + \ldots\right). \quad (5)$$

By slightly changing the length of the air path in the experiment, we modify the central frequency ω_0 and can extract the corresponding higher order dispersion of our silicon waveguide by fitting experimental data with Eq. (4). Our measurements are performed on a 2 cm long waveguide. The width and height of the silicon waveguide retreived from SEM are 840 and 230 nm, respectively. The dispersion measurements results are shown in Fig. 2. Figure 2(a) shows two examples of experimental interferograms obtained with the nanosecond supercontinuum (SC) source (top) and the CW ASE of the Cr^{2+}:ZnSe laser (bottom). The latter shows a very flat interferogram with high visibility (>10 dB). The SC source results show poorer spectral fringes and a stronger spectral dependence of the coherence function V, which is consistent with coherence studies of SC sources [17]. Both are fitted with Eq. (2) by truncating the dispersion expansion at the fourth order, as higher order dispersion didn't show improvement in the fitting. Extracted 2nd to 4th order dispersion coefficients for both sources are presented in Figs. 2(b)–2(d). We see measurable differences between the results for the two different sources we use. A parabolic fit of both second order dispersion (SOD) profiles confirms the difference in curvature by a factor 2. We believe the good agreement between the measured third (resp. fourth) order dispersion and the first (resp. second) order derivative of the parabolic fit indicates that this discrepancy is not due to measurement errors.

The reason for this is unclear, but the measurements with the SC source could be affected by the dispersion of the nonlinear parameter and the complex frequency dependence of the coherence function. However, we believe that the good agreement between both sources validate second and third order dispersion measurements with such a pulsed supercontinuum source, which allows to extend our measurement range in the spectral region of thulium-doped fiber sources where CW nonlinear conversion in silicon [18] and supercontinuum generation in amorphous silicon have been demonstrated [19]. Our measurements are compared to simulation results. Using a mode solver, we looked for the best fit of our experimental results within reasonable geometrical variations of the waveguide and found a good reproduction of the measured SOD for a waveguide of 217 nm × 860 nm (dotted line). There still is however a big discrepancy between simulations and experiment for the fourth order dispersion. This is consistent with previous

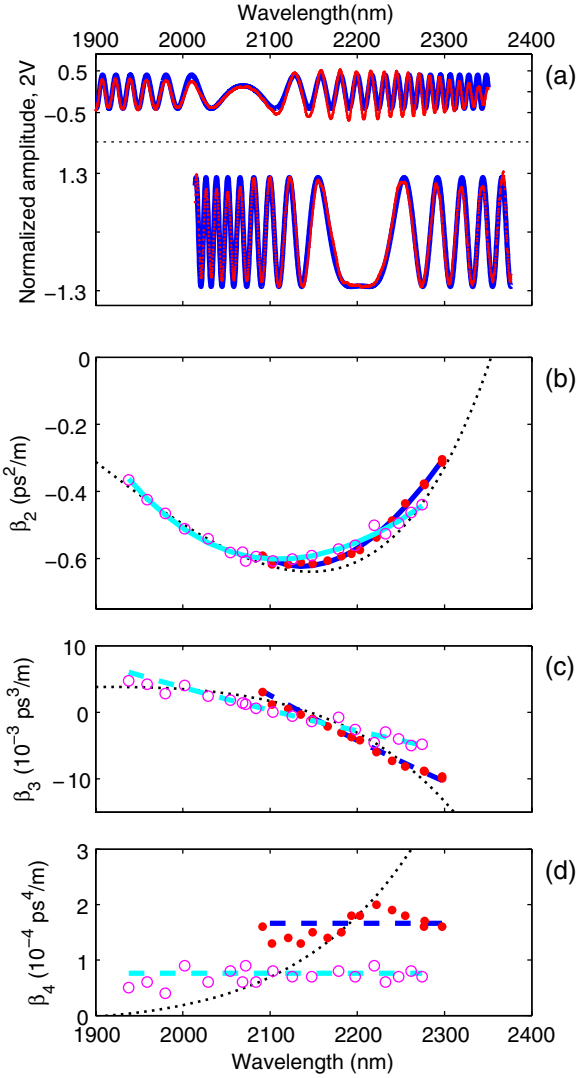

Fig. 2. (a) Example of two measured interferograms (red) with the pulsed (top) and CW (bottom) sources and corresponding fits (blue) using Eq (4). Experimental data has been smoothed by a Savitsky Golay filter. (b) Extracted SOD profile of our waveguide with the pulsed (circles) and CW (dots) sources. Both are fitted with a second-order polynomial for comparison with extracted higher order dispersion. Experimental results are compared with the SOD retrieved from mode solver simulations of a 860 nm × 217 nm (dotted) waveguide. [(c) resp. (d)] Extracted third (resp. fourth) order dispersion with the pulsed (open circles) and CW (dots) sources and comparison with first (resp. second) order derivative of the parabolic fit of figure (a) (dashed) and with third order dispersion (resp. fourth order dispersion) retrieved from simulations of a 860 nm × 217 nm waveguide (dotted).

experimental results of nonlinear conversion in similar waveguides, and we refer the reader to [5] for a discussion on possible causes. Our results confirm that the ZDW can be shifted to shorter wavelength from what is expected when designing the waveguide (with a targeted silicon thickness of 220 nm). This can be detrimental to nonlinear applications as some sources have limited tunability and working close to the ZDW is essential for applications such as frequency conversion and supercontinuum generation [6]. Moreover, the nonlinear losses of silicon significantly drop in this wavelength

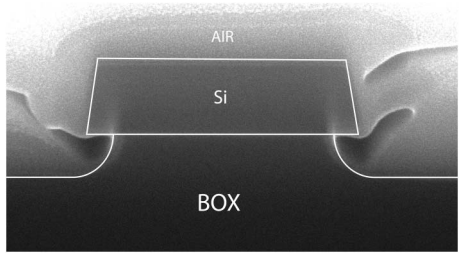

Fig. 3. SEM picture of our sample after full underetching with overlay corresponding to the waveguide profile used in simulations. Note that platina was deposited during SEM inspection. Width and height of the simulation profile are chosen to fit the measured SOD profile [see Fig. 2(b)]. The radius of the circular undercut is retrieved from a profilometer measurement.

range and pushing the anomalous region to longer wavelengths is essential for applications requiring CW pumping where free carrier absorption is detrimental. Tuning the ZDW to longer wavelengths can be achieved by underetching the waveguide, i.e., increasing the vertical confinement. It is performed by wet-etching the waveguide with a solution of diluted (1%) HF. Calibration measurements of the underetching with a profilometer showed an etching rate of 1.2 nm/ min. We underetched our waveguides in 2 steps of about 45 min. An etch depth of 55 and 113 nm was measured. A circular underetching profile was identified by SEM inspection (see Fig. 3). We performed a dispersion measurement on the underetched samples after both steps. We used only the CW

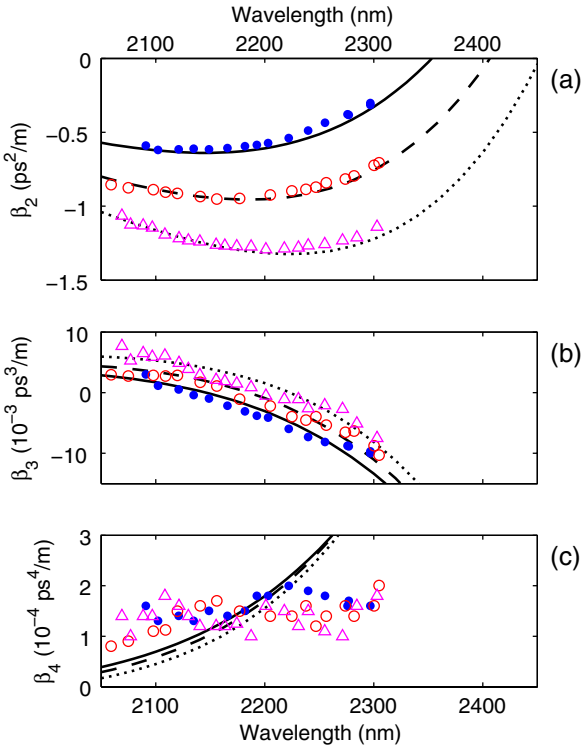

Fig. 4. Extracted second (a), third (b), and fourth (c) order dispersion of the waveguides after 0 nm (dots), 55 nm (open circles), and 113 nm (triangles) underetching. These results are compared with the corresponding dispersion retrieved from simulations of a 860 nm × 217 nm waveguide with 0 nm (full), 55 nm (dashed), and 113 nm (dotted) underetching.

ASE source as we are mainly interested in the longer wavelength range to show a shift of the ZDW.

Results are presented in Fig. 4 and compared to simulations of a waveguide with width and height extracted by fitting the SOD curve (before underetching) and using measured etch depths. An excellent agreement between measured and simulated SOD is found, showing a clear shift of the ZDW after underetching the sample. Very good agreement is also shown for the third-order dispersion. Moreover, both measurement and simulation of the fourth-order dispersion measurements show that the curvature of the SOD profile is left unchanged by the underetching. This confirms the potential of this simple technique for dispersion tuning. The possibility to slowly underetch should allow for very precise tuning of integrated parametric amplifiers. Using a cutback technique we have measured a small increase of propagation losses from 0.6 dB/cm before underetching to 0.9 dB/cm after 100 nm of underetching. Moreover, characteristics of high Q microresonators [20] and diffraction gratings for fiber-to-chip coupling for the short-wave infrared [21] were left unchanged when underetched up to 100 nm.

In conclusion we have demonstrated the measurement and tuning of second-to-fourth order dispersion of a silicon wire waveguide from 1950 to 2300 nm. We show good agreement with simulations of a waveguide with width and height within 5% from the values retrieved by SEM inspection. Dispersion tuning was performed by underetching and excellent agreement of the shift of the SOD profile between measurements and simulations is found. We believe further improvements, mainly reducing the overall loss of the measurement system, will allow to work without tapers and with longer waveguides. This should allow for very precise measurements of higher-order dispersion, which are essential to simulations of supercontinuum generation [22,23].

References

1. J. Leuthold, C. Koos, and W. Freude, Nat. Photonics **4**, 535 (2010).
2. H. K. Tsang, C. S. Wong, T. K. Liang, I. E. Day, S. W. Roberts, A. Harpin, J. Drake, and M. Asghari, Appl. Phys. Lett. **80**, 416 (2002).
3. X. Liu, J. B. Driscoll, J. I. Dadap, R. M. Osgood, S. Assefa, Y. A. Vlasov, and W. M. J. Green, Opt. Express **19**, 7778 (2011).
4. X. Liu, R. M. Osgood, Y. A. Vlasov, and W. M. J. Green, Nat. Photonics **4**, 557 (2010).
5. B. Kuyken, X. Liu, M. R. Osgood, Jr., R. Baets, G. Roelkens, and W. M. J. Green, Opt. Express **19**, 20172 (2011).
6. G. P. Agrawal, *Nonlinear Fiber Optics*, 4th ed. (Academic, 2006).
7. A. C. Turner, C. Manolatou, B. S. Schmidt, M. Lipson, M. A. Foster, J. E. Sharping, and A. L. Gaeta, Opt. Express **14**, 4357 (2006).
8. http://www.epixfab.eu.
9. B. Kuyken, X. Liu, G. Roelkens, R. Baets, J. Osgood, and W. M. J. Green, Opt. Lett. **36**, 4401 (2011).
10. P. A. Merritt, R. P. Tatam, and D. A. Jackson, J. Lightwave Technol. **7**, 703 (1989).
11. D. W. Kim, S. H. Kim, S. H. Lee, K.-H. Kim, J.-M. Lee, and E.-H. Lee, J. Lightwave Technol. **30**, 43 (2012).
12. S. Mas, J. Matres, J. Marti, and C. J. Oton, IEEE Photon. J. **4**, 825 (2012).
13. E. Dulkeith, F. Xia, L. Schares, W. M. J. Green, and Y. A. Vlasov, Opt. Express **14**, 3853 (2006).
14. X. Liu, W. M. J. Green, X. Chen, I.-W. Hsieh, J. I. Dadap, Y. A. Vlasov, and J. Osgood, Opt. Lett. **33**, 2889 (2008).
15. M. Erdmanis, L. Karvonen, M. R. Saleem, M. Ruoho, V. Pale, A. Tervonen, S. Honkanen, and I. Tittonen, J. Lightwave Technol. **30**, 2488 (2012).
16. E. Hecht and A. Zajac, *Optics* (Addison-Wesley, 2002).
17. J. M. Dudley and S. Coen, Opt. Lett. **27**, 1180 (2002).
18. R. K. W. Lau, M. Mnard, Y. Okawachi, M. A. Foster, A. C. Turner-Foster, R. Salem, M. Lipson, and A. L. Gaeta, Opt. Lett. **36**, 1263 (2011).
19. U. D. Dave, S. Uvin, B. Kuyken, S. Selvaraja, F. Leo, and G. Roelkens, Opt. Express **21**, 32032 (2013).
20. F. Leo, B. Kuyken, N. Hattasan, R. Baets, and G. Roelkens, *European Conference on Integrated Optics (ECIO 2012)*, Spain (2012), paper 156.
21. N. Hattasan, B. Kuyken, F. Leo, E. M. P. Ryckeboer, D. Vermeulen, and G. Roelkens, IEEE Photon. Technol. Lett. **24**, 1536 (2012).
22. L. Yin, Q. Lin, and G. P. Agrawal, Opt. Lett. **32**, 391 (2007).
23. F. Leo, S.-P. Gorza, J. Safioui, P. Kockaert, S. Coen, U. Dave, B. Kuyken, and G. Roelkens, "Dispersive wave emission and supercontinuum generation in a silicon wire waveguide pumped around the 1550 nm telecommunication wavelength," arXiv:1401.5713 (2014).